



HAL
open science

Modeling the salinity of an inland coastal brackish karstic spring with a conduit-matrix model

Bruno Arfib, Ghislain De Marsily

► **To cite this version:**

Bruno Arfib, Ghislain De Marsily. Modeling the salinity of an inland coastal brackish karstic spring with a conduit-matrix model. *Water Resources Research*, 2004, 40 (11), 10.1029/2004WR003147 . hal-01457521

HAL Id: hal-01457521

<https://hal.science/hal-01457521>

Submitted on 13 Jun 2018

HAL is a multi-disciplinary open access archive for the deposit and dissemination of scientific research documents, whether they are published or not. The documents may come from teaching and research institutions in France or abroad, or from public or private research centers.

L'archive ouverte pluridisciplinaire **HAL**, est destinée au dépôt et à la diffusion de documents scientifiques de niveau recherche, publiés ou non, émanant des établissements d'enseignement et de recherche français ou étrangers, des laboratoires publics ou privés.

Modeling the salinity of an inland coastal brackish karstic spring with a conduit-matrix model

B. Arfib

Laboratoire Chimie et Environnement, Université de Provence Aix-Marseille I, Marseille, France

G. de Marsily

Laboratoire de Géologie Appliquée, UMR CNRS 7619 Sisyphe, Université Pierre et Marie Curie, Paris, France

Received 2 March 2004; revised 2 July 2004; accepted 13 September 2004; published 10 November 2004.

[1] The salinity of an inland coastal brackish karstic spring is modeled on the basis of a simple concept of fluid exchange through head differences between a continuous porous matrix and a karst conduit. The coastal aquifer is reduced to an equivalent porous medium (matrix) naturally invaded by seawater, crossed by a single karst conduit where fresh water and brackish water mix in variable proportions and flow up into the spring. A new numerical model with an upwind explicit finite difference scheme, called salt-water intrusion in karst conduits (SWIKAC), was developed and successfully applied to the Almyros spring of Heraklio (Crete, Greece). The good fit of the model to the observed salinity in the spring validates the proposed conceptual model of salinization. It provides a quantitative description of the seawater intrusion inside the karst conduit. The results open up new perspectives for managing the fragile and precious fresh water resources in karstic coastal zones. *INDEX TERMS*: 1829 Hydrology: Groundwater hydrology; 1832 Hydrology: Groundwater transport; 1899 Hydrology: General or miscellaneous; *KEYWORDS*: karst modeling, coastal spring, conduit-matrix model, groundwater resource

Citation: Arfib, B., and G. de Marsily (2004), Modeling the salinity of an inland coastal brackish karstic spring with a conduit-matrix model, *Water Resour. Res.*, 40, W11506, doi:10.1029/2004WR003147.

1. Introduction

[2] Nowadays, models of flow and transport in porous coastal aquifers are widely used to quantify seawater intrusion due to natural conditions or to artificial withdrawal [e.g., Bear *et al.*, 1999]. There are many models which differ from each other mainly by the numerical methods used to solve the equations and by the assumption of miscible or immiscible fluids. Although these models can be successfully applied to porous media, they are hardly applicable to karstic systems.

[3] For karst aquifers, the problem becomes more complicated because no model is yet capable of representing the whole aquifer system without making drastic simplifying assumptions [Groves *et al.*, 1999]. The karstic system may be represented by an equivalent porous medium or a fracture network or a network of conduits or by a combination of all three [Dassargues and Brouyère, 1997; Halihan *et al.*, 2000; Worthington *et al.*, 2000]. When coastal karsts are investigated, in situ measurements should be used first in order to identify preferential flow paths and to find out the spatial distribution of the fresh and salt water within the aquifer [Moore *et al.*, 1992; Calvache and Pulido-Bosch, 1994; Howard and Mullings, 1996; Arfib *et al.*, 2000]. Thus the choice of a model depends on the objectives of the study and on the structure of the karstic system.

[4] Modeling examples of a coastal karst aquifer are rare. The existing simplified models are similar to those for continental karsts; they can be divided into five broad categories.

[5] 1. The simplest case is to consider the karstic system as an equivalent porous medium if the flow through the calcareous matrix is dominant. The karst conduits are represented by a zone of higher permeability [Wicks and Herman, 1995; Angelini and Dragoni, 1997; Quinn and Tomasko, 2000]. This type of representation is usually too unrealistic and, as Sasowsky [2000] has pointed out, few authors have adopted it.

[6] 2. The black box type models and the lumped models do not use a spatial division of the aquifer into meshes, but rather box reservoirs to represent the relationships between an input signal and an output of the system without explaining the physical processes behind these relationships [Bezes, 1976; Barrett and Charbeneau, 1997; Long and Derickson, 1999; Perrin *et al.*, 2001]. Generally, this method is based on the rainfall and the discharge, but it is not very relevant to our case since it cannot be used to study the mechanisms of saline intrusion in coastal karstic systems.

[7] 3. The karstic system can also be represented and modeled by a network of conduits if they have been individually identified. A pipe flow (non-Darcian) is calculated within the conduit [Halihan and Wicks, 1998; Jeannin, 2001]. The main disadvantage of this model is that it does not take into account the exchange between the network of conduits and its surrounding matrix (Figure 1). This is extremely restrictive and prevents the model from being applicable to a coastal aquifer where the saline inflow into

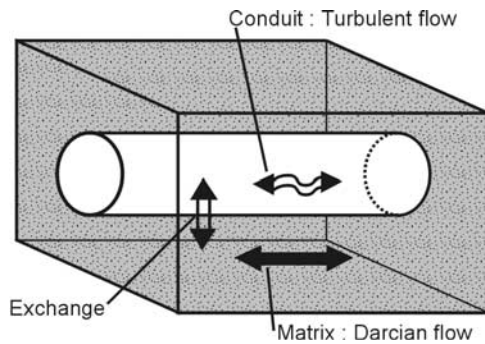


Figure 1. Conceptual sketch of the dual flow in a karst aquifer (conduit-matrix).

the conduit is diffuse. On the other hand, it makes it possible to take into consideration a localized entrance of salt water through another conduit connecting the network to the sea.

[8] 4. Modeling the flow in a discrete fracture network offers a solution that suits the karsts comparable to fractured media [Gylling *et al.*, 1999; Delle Rose *et al.*, 2000]. This method is not widely used because it needs extremely accurate and exhaustive information on the fracture network of the aquifer formation. It also requires long calculation times, but the growing speed of computers and the development of new numerical tools [e.g., Cravero and Fidelibus, 1999; Dershowitz and Fidelibus, 1999] should significantly increase the use of this method.

[9] 5. The last type of model considers a dual flow, combining a conduit network with a fissured matrix equivalent to a continuous porous medium. This type of model has been used on noncoastal karsts to simulate flow and transport [Mohrlök and Sauter, 1997; Kiraly, 1998; Annable and Sudicky, 1999]. For example, the software CAVE (Carbonate Aquifer Voids Evolution) uses this approach to model flow and transport and predict enlargement of karstic conduits in carbonate and gypsum [Clemens *et al.*, 1996, 1998; Liedl and Sauter, 1998; Bauer *et al.*, 1999; Birk *et al.*, 2003; Liedl *et al.*, 2003]. However, this software was not designed to model high-salinity variations such as in seawater intrusion and thus, in its present form, it is not suitable for coastal karst aquifers.

[10] A new numerical model of the fifth type, called saltwater intrusion in karst conduits (SWIKAC), was developed to study flow and transport in coastal karst aquifers influenced by seawater intrusion. Flow and transport are calculated for a single karstic conduit inside which fresh, then brackish, water flows. The brackish water results from the intrusion of seawater into the porous matrix surrounding the conduit, then exchanged with the conduit. This numerical model was designed to quantify the conceptual one describing the functioning of the coastal karstic aquifer supplying the Almyros spring of Heraklio (Crete, Greece) [Arfib *et al.*, 2002]. It simulates the salinity variation with time of the brackish spring, which is the main outlet of the system, using as input the continuously recorded discharge rate and water level at the spring. A few unknown physical parameters are calibrated on a 2-year history of the salinity at the spring. The model is used to estimate the depth of the saline inflow within the conduit. It can also be used as a tool to test the influence of changing

the head at the spring (e.g., by a small dam) on the salinity of the discharge water.

2. Conceptual Model of the Underground Flow in a Coastal Karst

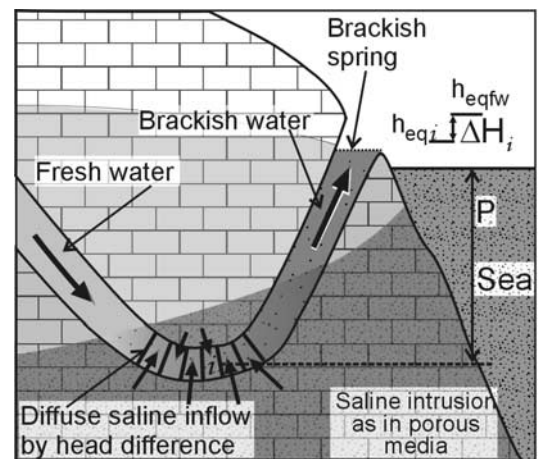
2.1. Dual Flow in the Saturated Zone of the Karst

[11] Flow in a karst aquifer can be divided between the two structural entities of karst: (1) the thinly fissured or porous limestone matrix, and (2) the karst conduits, generally located in highly fractured zones. The matrix is assumed similar to a continuous porous medium, with a Darcian flow, in contact with the karst conduits which are the preferential drains of the aquifer (or occasionally recharge it). In the conduits, the flow is rapid and mostly turbulent (Figure 1).

2.2. Saline Intrusion in a Coastal Karst Aquifer and Mechanism of Salinization of an Inland Brackish Spring: Example of the Almyros of Heraklio (Crete, Greece)

2.2.1. Theory

[12] Coastal aquifers, whether porous, fissured or karstic, discharge into the sea the freshwater recharged in the catchment area. The seawater, which is denser than the freshwater, enters into the aquifer below the freshwater as a saltwater wedge. A fragile equilibrium exists between the fresh and the salt waters, schematically represented by a sharp interface in continuous media. Its location can easily be estimated by analytical and numerical methods [Bear *et al.*, 1999]. However, in coastal karst aquifers, a karst conduit can locally cause a preferential flow of fresh or salt water, which modifies this equilibrium. When the conduit discharges at an inland spring, the salinity variations of the spring are functions of the exchange rates between the conduit containing some fresh water recharged in the inland part of the aquifer and the matrix filled by the intruded seawater (Figure 2). As water flows from the higher toward



P : Depth of the exchange zone
 h_{eqi} : Equivalent freshwater head in the conduit at point i
 h_{eqfw} : Equivalent freshwater head in the matrix at depth P
 ΔH_i : Conduit-matrix head difference at point i

Figure 2. Conceptual sketch of the mechanism of salinization by diffuse saline inflow into a coastal karst conduit (case of an unconfined aquifer).

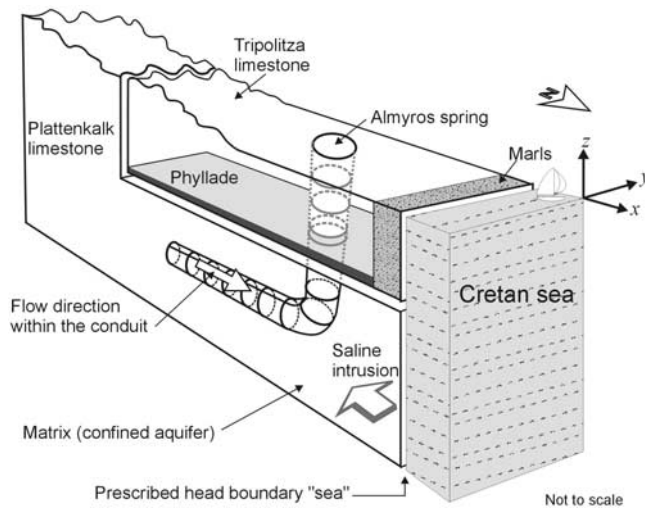


Figure 3. Schematic 3-D view of the coastal karstic aquifer of the Almyros of Heraklio spring.

the lower heads, the inflow of seawater from the matrix to the conduit is controlled by the head difference between the conduit and the matrix. The conduit can be considered as a pipe with a head distribution depending on the water levels at both ends, on the water density and on the turbulent head losses. Brackish and saline heads for the conduit and for the matrix zone intruded by seawater should be expressed as an equivalent reference freshwater head according to the following relation:

$$h_{eq} = \frac{\rho_{sw}}{\rho_{fw}} h_{sw} - \frac{\rho_{sw} - \rho_{fw}}{\rho_{fw}} z \quad (1)$$

where h_{eq} is the head of the saltwater expressed as an equivalent freshwater head, z is the elevation of the point of the head measurement taking the mean sea level as zero elevation, h_{sw} is the saltwater head in the aquifer containing a homogeneous fluid of density ρ_{sw} , ρ_{sw} is the density of the saltwater, and ρ_{fw} is the density of the reference freshwater.

[13] This conceptual model of saline intrusion in a coastal karst aquifer, although very intuitive and simplified, is not found in the literature because, so far, the matrix of the karst aquifer has not been taken into account when there is preferential flow in a conduit [Breznik, 1973]. This model is applicable to unconfined and confined aquifers. Only the numerical procedure changes according to the case. Its application to the confined aquifer of the Almyros of Heraklio is presented in the following. For this case, the coupling of aquifer flow to conduit flow is only in one direction, from the matrix to the conduit.

2.2.2. Example of the Almyros of Heraklio

[14] The broad karstic system of the Almyros of Heraklio, in Crete, was studied continuously during two years, beginning in September 1999 [Arfib *et al.*, 2000, 2002]. The goal of this study was to establish a conceptual model of the functioning of the system and to explain the salinization mechanism of the brackish Almyros spring with a future exploitation in mind.

[15] The aquifer covers 305 km² in the Ida massif, from the Sea of Crete to Mount Psiloritis (elevation 2456 m). The watershed basin consists of the two lower units of the

characteristic overthrust formations of Crete: the Cretaceous Plattenkalk and the Cretaceous Tripolitza limestone (Figure 3). The two limestone formations are locally separated by interbedded flysch or phyllade units that form an impervious layer [Bonneau *et al.*, 1977; Fassoulas, 1999] and may lead to a different flow behavior within the two karstic formations. The neotectonic activity has dissected these formations by large faults and fractures.

[16] The brackish Almyros of Heraklio spring is the only known outlet of the karst system. It flows out at 3 m above sea level, 1 km inland from the coast. Divers have explored the spring down to a depth of 90m but the conduit continues further. The water salinity is inversely correlated to the discharge rate. The water is brackish during low flow (in summer), up to a chloride content of 6 g L⁻¹, i.e., 23% of seawater, and is fresh during floods (in winter) when the flow rate exceeds 15 m³ s⁻¹ (14 days in 1999–2000 and 31 days in 2000–2001).

[17] The aquifer is recharged by fresh water from the mountains, which descends to an unknown depth through the confined aquifer of the Plattenkalk limestone where it acquires its salinity by seawater intrusion (Figure 3). The spring would be the largest water resource in the area, if it were possible to prevent it from being polluted by seawater. The main conduit is assumed to follow a preferential regional fracture zone directed north-south and perpendicular to the coastline. An impermeable marl formation prevents any direct communication between the spring and the sea down to a depth of several hundred meters.

[18] The numerical model SWIKAC was built in reference to the Almyros spring, using the conceptual conduit-matrix model presented in the previous paragraph and illustrated by Figure 4: (1) In the exchange zone between the matrix and the conduit, the conduit is assumed to be horizontal, at an unknown depth P (to be calibrated) below the sea level. (2) The brackish water flows up to the spring through a portion of an impermeable horizontal, then vertical, conduit over the length X in Figure 4. This length is also unknown and needs to be calibrated. This particular assumption derives from the observation of a systematic lag at the spring during any flood event between the beginning of the flow rate increase (pressure wave moving almost instantaneously) and the beginning of the salinity decrease (transport of salinity by the impermeable section of the conduit). During this time lag, it was observed that the same

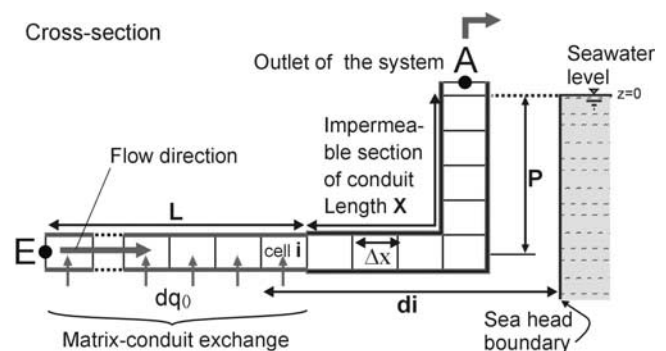


Figure 4. Cross section of the coastal karst aquifer showing a few parameters used in the SWIKAC model.

volume of water is discharged at the spring, around 770,000 m³, whatever the magnitude of the flood.

3. Numerical Model for Flow and Transport in a Coastal Karst Aquifer: The SWIKAC Model

[19] The observed functioning of the spring shows that, for this kind of system, a model that takes into account merely an equivalent porous medium, or merely a network of conduits, would not be suitable. It clearly shows the influence on the quality and quantity of the spring water of the heterogeneous structures, i.e., the karst conduit and its relationship with the surrounding matrix.

3.1. Theory

3.1.1. Turbulent Flow in the Conduits

[20] Where the network of karstic galleries can be identified, flow in the conduits follows the hydraulic laws for pipes. The flow may be laminar or turbulent, which is expressed by the Reynolds number (Re). The flow is laminar for Re lower than 2000 and is fully turbulent for Re higher than 4000 [e.g., *Chadwick and Morfett*, 1998].

$$Re = \frac{\rho u d_h}{\mu} \quad (2)$$

where ρ is the density of the fluid (kg m⁻³), μ is the viscosity of the fluid (Pa s), u is the mean velocity of the flow within the conduit (m s⁻¹), and d_h is the hydraulic diameter of the conduit (m).

[21] For flow in a conduit, we will use the following assumptions: (1) The flow is turbulent; (2) the temperature is constant; (3) the density of water is independent of the pressure but function of the salinity (incompressible fluid); (4) the fluid is Newtonian. In this case, the momentum conservation equation yields the classical Navier-Stokes equation [e.g., *de Marsily*, 1986]. We will further simplify Navier-Stokes by dropping the inertial term and by assuming that this inertial term can also be neglected in the definition of the hydraulic head. Let us briefly justify these two assumptions before proceeding to the special case of the Almyros spring. The observed maximum flow rate of the spring is on the order of 30 m³ s⁻¹. The equivalent diameter of the karstic conduit will be shown to be about 15 m. The average water velocity in the conduit at the maximum flow rate is thus on the order of 0.17 m s⁻¹. Although the Reynolds number is larger than 10⁶, the inertial term in the definition of the head ($u^2/2g$) is on the order 1.4×10^{-3} m, and can be ignored. For the inertial term in Navier Stokes, du/dt , to be compared to gravity, the fastest changes of flow rate with time, during storms, is from a low value to 30 m³ s⁻¹ in 40 hours. This gives a du/dt of 1.2×10^{-6} m s⁻², negligible compared to $g = 9.81$ m s⁻² in the vertical part of the conduit. In the horizontal part, this would also be true for any small angle of the conduit with the horizontal (e.g., 1.2×10^{-6} compared with 1.7×10^{-1} in m s⁻² for an angle of 1°). Similarly, the inertial term of the seawater seeping (with an almost zero initial velocity) into the conduit and reaching the brackish water velocity is neglected (for a unit mass of water going from a zero velocity to 0.17 m s⁻¹, the kinetic energy gain is 1.4×10^{-2} J, equivalent to a change in elevation of 1.5 mm). No other momentum conservation equation will be used; we will always assume that the

energy losses by friction are equal to the energy losses by gravity.

[22] With these assumptions, in turbulent flow, the head loss (h_f) is found to be experimentally function of the square of the velocity and can be expressed by the Darcy-Weisbach equation:

$$h_f = \frac{\lambda l u^2}{2g d_h} \quad (3)$$

where l is the length of the conduit, g is gravity, λ is the friction factor (dimensionless), u is the mean velocity of the flow, and d_h is the hydraulic diameter of the conduit.

[23] Nikuradse has shown by a series of experiments on artificially roughened pipes that the turbulence is also linked to the roughness of the conduit [e.g., *Chadwick and Morfett*, 1998]. He defined several types of turbulence depending on the roughness and the Reynolds number; for each type, a formula was established to calculate the friction factor λ . *Jeannin* [2001] proposes a relative roughness coefficient (kr) for the karstic system of the Hölloch cave (Switzerland) close to $kr = 0.25$; in such conditions, the classical Colebrook-White formula is not applicable. *Jeannin and Marechal* [1995] and *Jeannin* [2001] use the *Louis* [1974] formula, establish for turbulent flow in fractures, to calculate the friction factor λ :

$$\frac{1}{\sqrt{\lambda}} = -2 \log \left(\frac{kr}{1.9} \right) \quad (4)$$

Density does not appear in equations (3) and (4). Calculations with the Colebrook-White formula show that the density variations in the range of the values observed for freshwater and seawater (around 1000 to 1030 kg m⁻³) do not change the Reynolds number enough to modify the head loss value. *Louis'* formula and the Darcy-Weisbach equation were chosen for the SWIKAC model in the conduit. Furthermore, in the whole system, fluids are considered incompressible, and the mass balance equation reduces to the conservation of volumes. Freshwater and saltwater volumes are thus simply added, but the density of the mixture is, of course, taken into account to conserve salt mass balance.

3.1.2. Flow Between the Matrix (Confined Aquifer) and a Section of the Horizontal Conduit

[24] An estimate of the exchange flow rate of water between a porous matrix and a discrete fracture was proposed by *Barenblatt et al.* [1960] as a steady state flow (Q_e) proportional to the head difference between the matrix and the fracture (ΔH), the hydraulic conductivity of the matrix (K), the contact area between the fracture and the matrix (A) and a factor α [L⁻¹] which expresses the geometry of the fracture:

$$Q_e = \alpha AK \Delta H \quad (5)$$

A similar equation is used in SWIKAC to estimate the flow between the equivalent porous matrix and a horizontal karstic conduit in a coastal aquifer. The conduit is comparable to a horizontal well in a continuous aquifer with an inflow Q_e from the matrix to the conduit equivalent to a prescribed pumping rate (or an injection rate according

to the sign of Q_e). The time required for this radial flow to reach steady state is a function of the distance from the well to the boundary condition. We will assume that the aquifer is confined, and that the boundary is the sea (the aquifer is assumed infinite in the other direction). We will show later that the portion of the conduit where seawater seeps into the conduit lies about 5 km inland from the seashore. We can roughly estimate the time required by a converging flow in a 2-D confined aquifer to reach steady state. Using the image theory with the standard Theis solution [e.g., *de Marsily*, 1986], it is easy to find that steady state is obtained when the Theis variable v for the image well is close to 10^{-2} , i.e., when the Jacob approximation becomes valid. This is written:

$$v = \frac{R^2 S_s}{4Kt} < 0.01 \tag{6}$$

where R is the distance from a real well to its image well, symmetric with respect to the boundary (10 km), S_s is the specific storage coefficient (we assume a value of $3.5 \times 10^{-7} \text{ m}^{-1}$), K is the hydraulic conductivity (we take 10^{-3} m s^{-1}). One finds that $t > 10$ days is enough to reach steady state, or 100 days for $K = 10^{-4} \text{ m s}^{-1}$.

[25] However, we will assume that steady state conditions are valid at all times. This is likely to create an error for rapidly changing conditions in the conduit (the flow rate can go from a low to the maximum value in 40 hours, during a storm), but will, most likely, be valid for low-flow conditions. In reality, the α coefficient in equation (5) should be taken as time-dependent. Since this coefficient will be calibrated, one may say that the calibrated value represents a time-averaged value.

[26] For equation (5), the heads are expressed as equivalent freshwater heads (equation (1)). The head in the matrix is assumed constant at the “sea” boundary, i.e., where the matrix communicates with the sea (Figure 3). The head loss in the matrix between the “sea” boundary and the cylindrical karstic conduit is calculated in steady state by an analytical solution of the flow equation for radial convergent flow in a 2-D confined aquifer, the Dupuit solution. The solution for a confined aquifer was selected in the Almyros case, given the depth of the conduit and the geologic setting, but a different solution (e.g., a 3-D solution) or an unconfined one could be used if necessary. This solution, combined with the method of images [e.g., *de Marsily*, 1986] would be written, for a fully penetrating vertical well of radius r , flow rate dq , in an aquifer of transmissivity T (product of the hydraulic conductivity K by the thickness e of the aquifer), with a distance from the well to the sea of di :

$$\Delta h = \frac{dq}{2\pi T} \text{Ln} \left(\frac{2di}{r} \right) \tag{7}$$

Δh is the head difference between the sea level at the boundary and the head inside the well. The distance $2di$ comes from the fact that the distance of the “real” well to the “image” well is twice that from the well to the sea.

[27] Let us now assume that the well is not fully penetrating but has a length Δx instead of the full thickness e of the aquifer. As is classically done in well testing [e.g., *de*

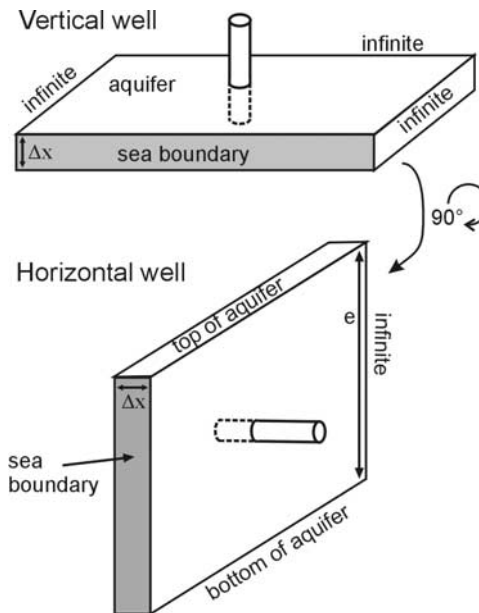


Figure 5. Analogy between a vertical pumping well and a horizontal pumping well in a vertical “slab” of thickness Δx .

Marsily, 1986], when the head is measured at the well bore, as is the case here, the transmissivity is taken as the product of K by Δx , and not by e . Let us now assume that this vertical well is turned so as to become a horizontal well of length Δx . Except for the case where the well is close to an impervious boundary, or where the aquifer is very thin, nothing has really changed in the flow pattern toward the well, the head drops occur mostly around the well, in the radial direction and the same expression can be used as an approximation. The “aquifer” now becomes a vertical slab of horizontal thickness Δx , with a prescribed head vertical boundary at the distance of the seashore and two horizontal no-flow boundaries at the top and bottom (Figure 5) when in reality the Dupuit formula applies if the “aquifer” is unbounded at the top and bottom. However, this is negligible if the thickness e of the aquifer is not too small ($e > 500 \text{ m}$ in the Almyros case). We can therefore write:

$$\Delta h = \frac{dq}{2\pi K \Delta x} \text{Ln} \left(\frac{2di}{r} \right) \tag{8}$$

We now divide the conduit into cells of length Δx , each of them considered as a well of radius r and length Δx and discharge dq_i . Reversing equation (8):

$$dq_i = \frac{2\pi K \Delta x \Delta h}{\text{Ln} \left(\frac{2di}{r} \right)} \tag{9}$$

where $\Delta h = h_{\text{eqfw}} - h_{\text{eq}i}$, as illustrated in Figure 2, $h_{\text{eq}i}$ is the equivalent freshwater head within the conduit at cell i calculated from the head loss equations (3) and (4) and the definition of the equivalent head (1); h_{eqfw} is the equivalent freshwater head in the aquifer at the sea boundary, calculated at the depth of the conduit (unknown, but will be shown to be on the order of 500 m) with (1), for a water

temperature of 15°C, $\rho_{fw} = 999.1 \text{ kg m}^{-3}$, and in the Sea of Crete, $\rho_{sw} = 1029.1 \text{ kg m}^{-3}$.

[28] We finally assume that the individual “horizontal wells” of length Δx have no influence on each other. This is also an approximation, but consistent with assuming that each well is assigned a “section” of aquifer of thickness Δx (Figure 5): if the conduit were parallel to the seashore, of infinite length, and if the inflow rate were constant over each length Δx , it would be exact. For the case study of the Almyros, the conduit is more likely to be perpendicular to the boundary. Thus this expression is only approximate, but the variable distance to the sea is incorporated since the distance d_i is variable.

3.1.3. Solute Transport

[29] In a karstic aquifer, solute transport is controlled by two major migration mechanisms: advection and hydrodynamic dispersion, combined in the classical advection-dispersion equation. This equation applies to both the conduit network and the matrix. To simplify the SWIKAC program, we focused only on the solute transport within the conduit because of the inflow of a solution with a constant concentration from the matrix to the conduit. We assumed that the salinity of the water in the matrix is equal to that of the sea.

[30] The transport is calculated in 1-D, in the direction of the conduit, by an upwind explicit finite difference scheme. This kind of numerical scheme, also called “mixing cell model”, has been used several times to simulate transport in porous aquifers [Van Ommen, 1985; Bajracharya and Barry, 1994; Harrington et al., 1999] and in karst aquifers [e.g., Clemens et al., 1996; Tezcan, 1998], and compared with the results of a numerical Crank-Nicholson solution of the true advection-dispersion equation [Bajracharya and Barry, 1993].

[31] The mixing cell model is composed of a discrete number of cylindrical cells of length Δx and radius r . It assumes instant mixing and a homogeneous concentration in each cell. The calculations are made at each time step, of length Δt . The concentration calculation ($C_{(i,n\Delta t)}$) in a cell with a suffix i (increasing in the flow direction) at time $n\Delta t$ is obtained by adding to the initial mass of solute in the cell the incoming mass of solute from the upstream section, and from the walls of the conduit, and subtracting the mass of solute leaving the cell at the downstream end:

$$C_{(i,n\Delta t)} = \frac{\text{Initial Mass} + \text{Entering Mass} - \text{Outgoing Mass}}{\text{Volume}} \quad (10)$$

The initial mass is $C_{(i,(n-1)\Delta t)} \pi r^2 \Delta x$, the entering mass is $Q_{(i-1,n\Delta t)} C_{(i-1,(n-1)\Delta t)} \Delta t + dq_{(i,n\Delta t)} Cl_{sw} \Delta t$, and the outgoing mass is $Q_{(i,n\Delta t)} C_{(i,(n-1)\Delta t)} \Delta t$. The water mass balance gives $Q_{(i-1,n\Delta t)} + dq_{(i,n\Delta t)} = Q_{(i,n\Delta t)}$ with $Q_{(i,n\Delta t)}$: the total outflow rate of the cell i at the time $n\Delta t$ to the cell $(i+1)$, $dq_{(i,n\Delta t)}$: the inflow rate of water calculated with equation (9) from the matrix to the conduit in cell i at time $n\Delta t$, Cl_{sw} : the chloride content of the incoming matrix water, assumed constant through time and equal to that of seawater.

[32] We then find

$$C_{(i,n\Delta t)} = C_{(i,(n-1)\Delta t)} - \frac{Q_{(i,n\Delta t)} \Delta t}{\Delta x \pi r^2} (C_{(i,(n-1)\Delta t)} - C_{(i-1,(n-1)\Delta t)}) - \frac{dq_{(i,n\Delta t)} \Delta t}{\Delta x \pi r^2} (C_{(i-1,(n-1)\Delta t)} - Cl_{sw}) \quad (11)$$

In this model, we assume instantaneous mixing between freshwater and seawater. In reality, two mechanisms govern the mixing: (1) stratification, due to the density difference, which retards mixing, as observed e.g., in estuaries, (2) turbulence, which, on the contrary, accelerates mixing. Molecular diffusion at the freshwater/saltwater interface is considered negligible.

[33] In a karstic system, we believe that the turbulence is enhanced by the complex and rough geometry of the conduits. The high calibrated value of the relative roughness coefficient kr (1.1, see below) is a strong indication of high turbulence. We therefore neglected stratification, and assumed instant mixing, but, as will be shown below, this may introduce an error, especially during low flow.

[34] The mixing cell model calculates an explicit solution of the pure advective solute transport equation, with an upwind scheme of the spatial concentration variations. This solution is numerically stable if the Courant number (N_{Co}) is lower than or equal to 1:

$$N_{Co} = \left| \frac{u \Delta t}{\Delta x} \right| \leq 1 \quad (12)$$

where u is the average velocity in the conduit, with flow rate Q , in any cell i and at time $n\Delta t$:

$$u = \frac{Q}{\pi r^2} \quad (13)$$

We will select Δt and Δx so that this condition is always met, for each cell.

[35] The longitudinal hydrodynamic dispersion coefficient of the classical advection-dispersion equation (D_h) is not explicitly included in equation (11). However, the model generates some numerical dispersion (D_n), which has the same mixing properties as the true hydrodynamic dispersion. The total numerical dispersion D_n is the sum of the dispersion due to the upwind in space and to the explicit form in time of equation (11):

$$D_n = \frac{u \Delta x}{2} - \frac{u^2 \Delta t}{2} = \frac{u \Delta x}{2} (1 - N_{Co}) \quad (14)$$

The choice of Δt and Δx will therefore define the dispersion included in the model.

3.2. SWIKAC Model

[36] The SWIKAC model was developed for this study on Matlab 6. It uses the conceptual model presented previously, with the following procedure. The flow and transport equations are calculated starting from the spring, in the direction opposite to the flow. For each time step $n\Delta t$, a first loop calculates the head distribution within the impermeable section of the conduit of length X in Figure 4, with the discharge and the head measured at the Almyros spring every 30 min. Heads expressed as equivalent freshwater heads (h_{eqi}) are calculated for each cell with equations (1), (3), and (4), with the discharge to the downstream cell. In the horizontal section of the conduit, where seawater flows in, the head in the matrix is assumed constant, equal to the head at the sea level expressed as an equivalent freshwater head with equation (1) (h_{eqfw}). A second loop calculates, for each cell in the

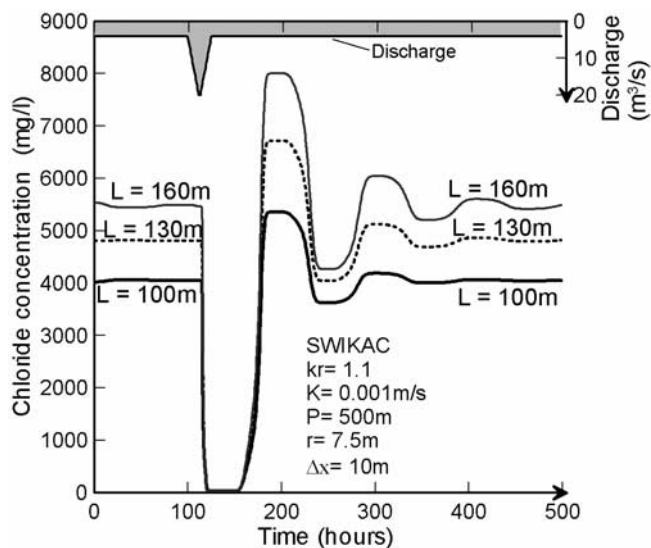


Figure 6. Chloride concentration at the spring for different lengths (L) of the saltwater inflow zone into the conduit.

horizontal section: the discharge to the downstream cell (Q_i), then the head in the conduit (h_{eqi}) with the water density of the cell at the previous time step ($(n-1)\Delta t$), then the seawater inflow with equation (9) (dq_i), and then finally, the chloride concentration, homogeneous in the cell, with equation (11) (C_i). For each time step, the loop stops when the length L (Figure 4) of the seawater inflow zone is reached. In case an inverse head gradient is calculated ($\Delta h < 0$ in equation (9)), the flow rate dq_i is taken as zero.

3.2.1. Data and Fitting Parameters

[37] The input data of the model are the discharge rate and the level of the water at the spring, recorded continuously. At present, the model is not meant to predict the flow rate of the spring but only to explain its salinity variations, given the values of three fitting parameters: P is the depth (unknown) below the sea level of the conduit zone where the saltwater penetrates into the conduit (Figure 4). This value is used to calculate the equivalent freshwater heads (equation (1)); it must be sufficiently deep to observe any inflow of seawater into the conduit. L is length over which the seawater enters the conduit. Finally, kr is mean relative roughness coefficient of the conduit.

[38] The fitting of the model is done by a trial-and-error procedure. It consists in minimizing the difference between the measured and calculated salinity versus time, at the spring. The following constants must also be specified: K is the mean hydraulic conductivity of the matrix surrounding the conduit over the length L . From equation (9), the seawater inflow will be proportional to K . Here r is the mean radius of the conduit. It influences the head losses within the conduit, the flow velocity and the area of exchange between the matrix and the conduit. X is the distance between the spring and the end of the seawater inflow zone within the conduit (Figure 4); r and X are linked by the volume stored in the conduit, known to be around $770,000 \text{ m}^3$ from the lag time.

3.2.2. Influence of the Model Fitting Parameters:

L and kr

[39] The length L can directly compensate for the permeability and diameter variations, as shown by equation (9),

where the length Δx , the hydraulic conductivity K and the logarithm of the conduit radius r are all positively related to the flow entering the conduit. Only parameters L and kr were found to be sensitive in the calibration.

[40] In the following tests, we used a Δx of 10 m and a Δt of 60 s. Figure 6 shows the effect of the length L on the chloride concentration predicted at the spring when the total discharge (at the spring) rises from 4 to $20 \text{ m}^3 \text{ s}^{-1}$ in 12 hours and then returns to $4 \text{ m}^3 \text{ s}^{-1}$. The greater the length L , the higher is the chloride concentration at the discharge rate of $4 \text{ m}^3 \text{ s}^{-1}$. However, when the discharge rate is $20 \text{ m}^3 \text{ s}^{-1}$, the length L variations have no effect on the simulated chloride concentration (time 120 to 155 on Figure 6).

[41] Figure 7 shows the effect of the relative roughness coefficient kr on the chloride concentration predicted at the spring when the total discharge (at the spring) rises from 4 to $20 \text{ m}^3 \text{ s}^{-1}$, and returns to $4 \text{ m}^3 \text{ s}^{-1}$. The dash plot is the same in Figures 6 and 7. A low relative roughness coefficient always gives a simulated concentration higher than zero when the discharge rate is high. On the other hand, a high kr increases the time during which the water is fresh (concentration close to zero). The high coefficient ($kr = 1.5$ in this example) also decreases the initial water salinity during the low-flow period.

[42] To summarize, the length L affects the rate of seawater inflow within the conduit during the low-flow periods, whereas the relative roughness coefficient kr affects the minimum value of the chloride concentration during the high-flow periods (floods).

[43] The salinity oscillations simulated after 175 hours in Figures 6 and 7 are not numerical artifacts. They have a physical explanation, linked to two factors: (1) the density of the water is variable within the conduit, and (2) the conduit geometry is divided into a horizontal part where the seawater enters and a vertical part close to the spring (Figures 3 and 4). The salinity variation in the vertical part of the conduit (when fluids with changing density progress vertically) generates some head variations within the conduit (equation (1)). These variations affect the seawater

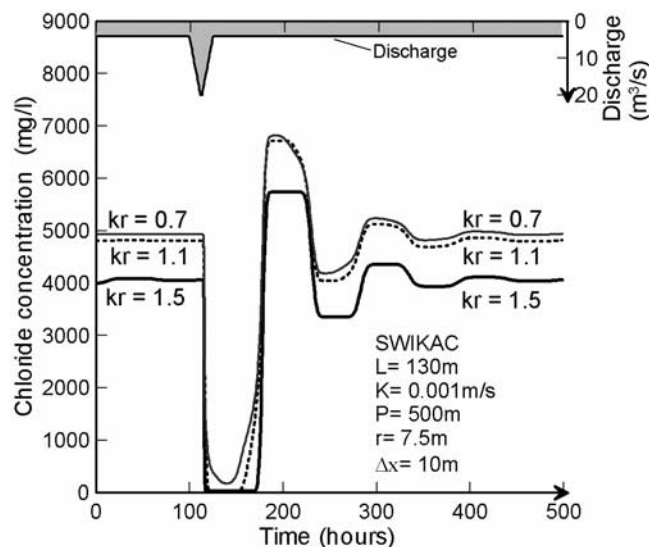


Figure 7. Chloride concentration at the spring for different values of the roughness coefficient (kr) of the conduit.

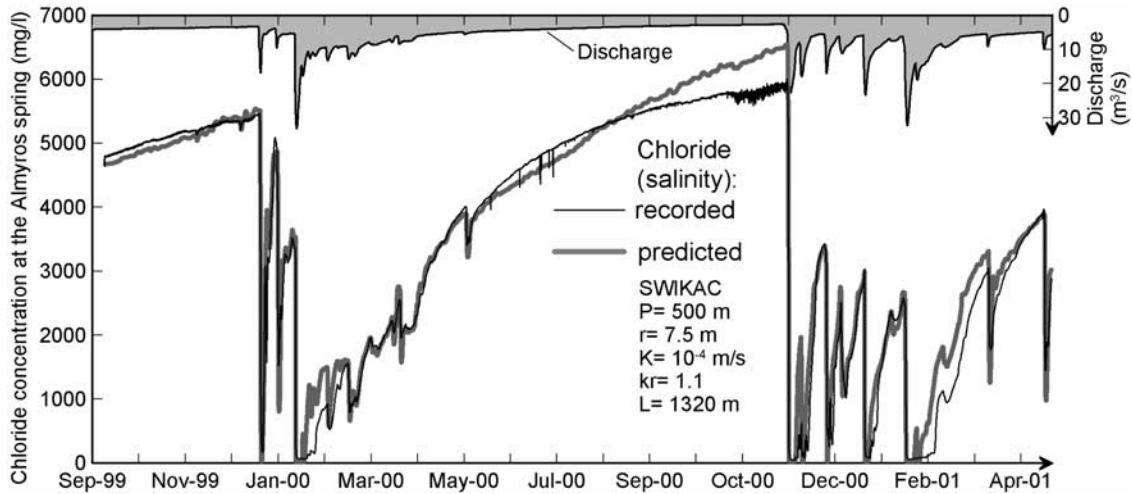


Figure 8. Recorded chloride concentration and that predicted with the SWIKAC model at the Almyros of Heraklio spring (Crete).

inflow (equations (5) and (9)), regardless of the discharge variations at the spring. The massive inflow of seawater into the conduit at the end of a flood generates an increase in head inside the conduit with a time lag due to the transport process. This head increase is linked to the density increase of the water flowing in the vertical part of the conduit. When the head in the conduit increases, the head difference between the conduit and the matrix decreases (equations (5) and (9)). The seawater inflow decreases and so does the salinity in the conduit. When, in turn, this water with a lower salinity and density arrives in the vertical part of the conduit, it reduces the head in the conduit, a new cycle of oscillations begins with a new increase in the inflow of seawater. These oscillations of the concentration die down naturally with time because of the mixing in the conduit of the fluids with variable density (no inertial effects are involved), and they are actually observed, but with a smaller amplitude, in natural conditions at the Almyros spring with some smoother discharge rate variations in time.

4. Application to a Time Period

[44] The chloride concentration of the Almyros spring of Heraklio was simulated during two years (Figure 8). The model gives very good results, close to the recorded concentration values, for several sets of parameters P , K , r , L and kr . The values for K and r were selected from previous work [Arfib, 2001]. Δx and Δt were kept between 10 to 20 m and 10 to 60 s.

[45] The mean hydraulic conductivity K of the matrix is estimated at between 10^{-4} m s^{-1} and 10^{-3} m s^{-1} . This uncertainty influences only the calibration of the length L (see section 3.2.2). A smaller value of K ($K = 10^{-5} \text{ m s}^{-1}$) requires an unrealistic value of L , the length of the zone of saline inflow along the conduit (over 10 km). The conduit radius, r , assumed constant in the numerical model, was tested for values between 5 and 10 m, which corresponds to a distance (X in figure 4) from the spring to the seawater inflow zone in the conduit of between 2.5 and 10 km.

[46] The model shows that the depth P must be at least 400 m below sea level. If less, the simulated salinity is systematically underestimated by the model. Any value of P

greater than 400 m gives good results close to the measurements. However, values of P greater than 800 m were not tested, because they do not, a priori, have any geological justification. In order to determine the most likely value of the depth P , a second series of data recorded at the spring with different head conditions was used. The second set of concentration and discharge data results from an experiment conducted at the spring in 1987, when the level of the spring was artificially raised by a dam to a level 5 m above the natural mean level. The depth P of the horizontal seawater inflow zone along the conduit (Figure 4), which allows the two series of observations to be fitted, is estimated to be 500 m.

[47] Figure 8 illustrates the results produced by the SWIKAC model for a conduit depth of 500 m, a radius of 7.5 m and a matrix hydraulic conductivity of 10^{-4} m s^{-1} . The length of the seawater inflow zone along the conduit is then 1320 m, starting at a distance of 4,350 m from the spring, and the relative roughness coefficient kr is 1.1. This high roughness coefficient could be interpreted as an equivalent roughness coefficient. It includes the roughness of the conduit itself and some special features of the conduit such as: fallen blocks, nonconstant diameter, bends, etc. The model simulates very well the general shape of the chloride concentration with time. Note that the simulation is good for the two seasonal cycles, although the meteorological conditions were very different from one cycle to the other (1999–2000: rainy year, 2000–2001 dry year). Two periods appear to be poorly simulated, but this can be explained by the simplicity of the model and gives some further information on the functioning of the karstic system. They are (1) the period following strong freshwater floods (January 2000, February–March 2001), when the model does not account for the expulsion of freshwater into the matrix outside the conduit and the return of this freshwater which dilutes the tail of the flood, and (2) the end of the low-water period when the measured salinity is lower than the simulated one (August–November 2000), which might be explained by density stratification phenomena of freshwater-saltwater in the conduit. We have indeed observed, in a preliminary laboratory experiment, that the saltwater accumulates at the bottom of the conduit in the

horizontal portion of the conduit and moves at a lower velocity than the overlying freshwater [Arfib and Ganoulis, 2004]. Turbulence is not sufficient to fully mix the two fluids, which are separated by an interface, through which diffusion (and local dispersion) generates a flux of salt to the overlying freshwater, but at a lower rate than if complete mixing were taking place. This interface certainly disappears in the vertical portion of the conduits, but the saltwater, which has a lower velocity than the freshwater, enters the vertical conduit at a reduced rate.

5. Conclusions

[48] Brackish karstic springs near the coast, or even emerging in the sea, are attracting increasing attention especially along the Mediterranean coast [e.g., *Bakalowicz et al.*, 2003], but also elsewhere in the world, because of the growing demand for freshwater. The results presented in this paper open up some new perspectives for the management of the fragile and precious fresh water resource of coastal karstic zones. We show that, in certain cases, distributed modeling of the solute transport in a coastal karst aquifer is possible. The SWIKAC model developed for the specific case of the Almyros of Heraklio spring, uses simple numerical methods and suggests some quantitative information on the mechanisms of groundwater salinization in a coastal karst aquifer. However, it is based on a set of simplifying assumptions, such as a single conduit with a constant diameter, a high and constant roughness coefficient and a constant hydraulic conductivity of the matrix. The simulation with the data of the Almyros of Heraklio spring shows two distinct periods: (1) one very close to the observations, which “validates” the conceptual model of the aquifer, and (2) two others with underestimates or overestimates of the salinity which indicate the existence of other physical phenomena that are not taken into account by the model or, alternatively, the effect of some of our simplifying assumptions.

[49] The way in which the seawater flows into the conduit, its depth, and its distance to the spring are essential elements to be considered when a freshwater exploitation scheme is designed. A possibility could be, for example, designing a dam at the spring in order to increase the head in the conduit and decrease the seawater inflow in the conduit. Using SWIKAC, we found that a dam with an elevation of 15 m above the present mean sea level would prevent any saltwater intrusion at the Almyros; however, it may be debatable whether such an increase in head might not, in the long term, open or reopen other conduits discharging the karstic system elsewhere. Other possibilities could be boreholes pumping saltwater from the matrix in the vicinity of the permeable conduit to decrease the saltwater head and its flow into the conduit and withdrawal in the karstic conduit upstream from the exchange zone, before the saltwater inflow. The last two options require that the precise location of the conduit be identified, which is presently very difficult as the estimated depth is 500 m. Then, even if the spring water is not totally fresh (e.g., 23% of seawater at the Almyros spring in summer), reverse osmosis can be used to make it drinkable, at a much lower cost than that of treating seawater. The SWIKAC model could be applied to such karst systems to predict the salinity variation as a function of the flow rate, provided that these

variations are inversely correlated to the discharge, and that salinity and flow rate data have been recorded, which unfortunately is still rarely the case.

[50] **Acknowledgment.** The authors wish to express their gratitude to the European Commission, which provided a Marie Curie scholarship to the first author for his Ph.D. thesis, to Professor Jacques Ganoulis (University of Thessaloniki, Greece) with the help of whom all the field work was accomplished, and to two anonymous reviewers who helped improve an earlier draft of this article.

References

- Angelini, P., and W. Dragoni (1997), The problem of modeling limestone springs: The case of Bagnara (north Apennines, Italy), *Ground Water*, 35(4), 612–618.
- Annable, W. K., and E. A. Sudicky (1999), On predicting contaminant transport in carbonate terrains: Behavior and prediction, in *Karst Modeling, Spec. Publ. 5*, pp. 133–145, Karst Waters Inst., Charles Town, W. V.
- Arfib, B. (2001), Etude des circulations d’eaux souterraines en aquifères karstiques côtiers: Observations et modélisation de la source saumâtre Almyros d’Héraklion, Crète (Grèce), 343 pp., Ph.D. thesis, Univ. of Paris 6, Paris.
- Arfib, B., and J. Ganoulis (2004), Modélisation physique de l’intrusion d’eau de mer dans un aquifère karstique: Cas de l’Almyros d’Héraklion (Crète), C.R.A.S., *Geosciences*, 336, 999–1006.
- Arfib, B., G. de Marsily, and J. Ganoulis (2000), Pollution by seawater intrusion into a karst system: New research in the case of the Almyros source (Heraklio, Crete, Greece), *Acta Carsol.*, 29(1), 15–31.
- Arfib, B., G. de Marsily, and J. Ganoulis (2002), Les sources karstiques côtières en Méditerranée: Etude des mécanismes de pollution saline de l’Almyros d’Héraklion (Crète), observations et modélisation, *Bull. Soc. Geol. Fr.*, 173(3), 53–61.
- Bajracharya, K., and D. A. Barry (1993), Mixing cell models for nonlinear nonequilibrium single species adsorption and transport, *Water Resour. Res.*, 29(5), 1405–1413.
- Bajracharya, K., and D. A. Barry (1994), Note on common mixing cell models, *J. Hydrol.*, 153, 189–214.
- Bakalowicz, M., P. Fleury, N. Döerfliger, and J. L. Seidel (2003), Coastal karst aquifers in Mediterranean regions: A valuable groundwater in complex aquifers, in *Tecnologia de la Intrusion de Agua de mar en acuíferos costeros: Paises Meditarranos* (TIAC), pp. 125–128, Inst. Geol. et Minero de Esp., Madrid.
- Barenblatt, G. E., I. P. Zheltov, and I. N. Kochina (1960), Basic concepts in the theory of homogeneous liquids in fractured rocks, *J. Appl. Math. Mech.*, 24, 1286–1303.
- Barrett, M., and R. Charbeneau (1997), A parsimonious model for simulating flow in a karst aquifer, *J. Hydrol.*, 196, 47–65.
- Bauer, S., S. Birk, R. Liedl, and M. Sauter (1999), Solutionally enhanced leakage rates of dams in karst regions, in *Karst Modeling, Spec. Publ. 5*, pp. 158–162, Karst Waters Inst., Charles Town, W. V.
- Bear, J. A., H.-D. Cheng, S. Sorek, I. Herrera, and D. Ouazar (Eds.) (1999), *Seawater Intrusion in Coastal Aquifers*, 625 pp., Kluwer Acad., Norwell, Mass.
- Bezes, C. (1976), Contribution à la modélisation des systèmes aquifères karstiques; Etablissement du modèle BEMER, son application à quatre systèmes karstiques du midi de la France, doctoral thesis, 135 pp., Cent. d’Etudes et de Rech. Géodyn. et Astron., Univ. des Sci. et Techniques du Languedoc, Montpellier 2, Montpellier, France.
- Birk, S., R. Liedl, M. Sauter, and G. Teutsch (2003), Hydraulic boundary conditions as a controlling factor in karst genesis: A numerical modeling study on artesian conduit development in gypsum, *Water Resour. Res.*, 39(1), 1004, doi:10.1029/2002WR001308.
- Bonneau, M., J. Angelier, M. Epting, and J. Auboin (1977), Réunion de la Société géologique de France en Crète, *Bull. Soc. Geol. Fr.*, 7(1), 87–102.
- Breznik, M. (1973), The origin of the brackish karstic springs and their development, *Geologija*, 16, 84–183.
- Calvache, M. L., and A. Pulido-Bosch (1994), Modeling the effects of saltwater intrusion dynamics for a coastal karstified block connected to a detrital aquifer, *Ground Water*, 32(5), 767–777.
- Chadwick, A., and J. Morfett (1998), *Hydraulics in Civil and Environmental Engineering*, 3rd ed., 600 pp., E & FN Spon, New York.
- Clemens, T., D. Hückinghaus, M. Sauter, R. Liedl, and G. Teutsch (1996), A combined continuum and discrete network reactive transport model for the simulation of karst development, in *ModelCare 96, Calibration and Reliability in Groundwater Modelling*, edited by K. Kovar and P. Van der Heijde, *IAHS Publ.*, 237, 309–318.

- Clemens, T., D. Hückinghaus, M. Sauter, R. Liedl, and G. Teutsch (1998), Simulation of the evolution of maze caves, in *Modelling in Karst Systems, Bull. Hydrogeol. Neuchatel*, 16, 201–209.
- Cravero, M., and C. Fidelibus (1999), A code for scaled flow simulations on generated fracture networks, Short note, *Comput. Geosci.*, 25, 191–195.
- Dassargues, A., and S. Brouyère (1997), Are deterministic models helpful to delineate groundwater protection zones in karstic aquifers?, in *Karst Water and Environmental Impacts*, pp. 109–117, A. A. Balkema, Brookfield, Vt.
- Delle Rose, M., A. Federico, and C. Fidelibus (2000), A computer simulation of groundwater salinization risk in Salento peninsula (Italy), in *Proceedings of Risk Analysis 2000, Bologna, Italy*, edited by C. A. Brebbia, 10 pp., Wessex Inst. of Technol., Ashurst, U. K.
- de Marsily, G. (1986), *Quantitative Hydrogeology*, 440 pp., Academic, San Diego, Calif.
- Dershowitz, W. S., and C. Fidelibus (1999), Derivation of equivalent pipe network analogues for three-dimensional discrete fracture networks by the boundary element method, *Water Resour. Res.*, 35, 2685–2691.
- Fassoulas, C. (1999), The structural evolution of the central Crete: Insight into the tectonic evolution of the south Aegean (Greece), *J. Geodyn.*, 27, 23–43.
- Groves, C., J. Meiman, and A. D. Howard (1999), Bridging the gap between real and mathematically simulated karst aquifers, in *Karst Modeling, Spec. Publ. 5*, pp. 197–202, Karst Waters Inst., Charles Town, W. V.
- Gylling, B., L. Moreno, and I. Neretnieks (1999), The channel network model—A tool for transport simulations in fractured media, *Ground Water*, 37(3), 367–375.
- Halihan, T., and C. Wicks (1998), Modeling of storm responses in conduit flow aquifers with reservoirs, *J. Hydrol.*, 208, 82–91.
- Halihan, T., R. E. Mace, and J. M. Sharp Jr. (2000), Flow in the San Antonio segment of the Edwards Aquifer: Matrix, fractures or conduits?, in *Groundwater Flow and Contaminant Transport in Carbonate Aquifers*, edited by I. D. Sasowsky and C. M. Wicks, pp. 129–146, A. A. Balkema, Brookfield, Vt.
- Harrington, G. A., G. R. Walker, A. J. Love, and K. A. Narayan (1999), A compartmental mixing-cell approach for the quantitative assessment of groundwater dynamics in the Otway Basin, South Australia, *J. Hydrol.*, 214(1–4), 49–63.
- Howard, K. W. F., and E. Mullings (1996), Hydrochemical analysis of groundwater flow and saline incursion in the Clarendon basin, Jamaica, *Ground Water*, 34(5), 801–810.
- Jeannin, P.-Y. (2001), Modeling flow in phreatic and epiphreatic karst conduits in the Hölloch cave (Muotatal, Switzerland), *Water Resour. Res.*, 37(2), 191–200.
- Jeannin, P.-Y., and J.-C. Marechal (1995), Lois de perte de charge dans les conduits karstiques: Base théorique et observations, *Bull. Hydrogeol. Neuchatel*, 14, 149–176.
- Kiraly, L. (1998), Modelling karst aquifers by the combined discrete channel and continuum approach, in *Modelling in Karst Systems, Bull. Hydrogeol. Neuchatel*, 16, 77–98.
- Liedl, R., and M. Sauter (1998), Modelling of aquifer genesis and heat transport in karst systems, in *Modelling in Karst Systems, Bull. Hydrogeol. Neuchatel*, 16, 185–200.
- Liedl, R., M. Sauter, D. Hückinghaus, T. Clemens, and G. Teutsch (2003), Simulation of the development of karst aquifers using a coupled continuum pipe flow model, *Water Resour. Res.*, 39(3), 1057, doi:10.1029/2001WR001206.
- Long, A. J., and R. G. Derickson (1999), Linear systems analysis in a karst aquifer, *J. Hydrol.*, 219, 206–217.
- Louis, C. (1974), Introduction à l'hydraulique des roches, *Bull. Bur. Rech. Geol. Min. Sect. 3, 4*, 283–356.
- Mohrlok, U., and M. Sauter (1997), Modelling groundwater flow in a karst terrane using discrete and double-continuum approaches—Importance of spatial and temporal distribution of recharge, paper presented at 6th Conference on Limestone Hydrology and Fissured Media, Univ. de Franche-Comté, La Chaux-de-Fonds, France.
- Moore, Y. H., R. K. Stoessell, and D. H. Easley (1992), Freshwater/seawater relationship within a groundwater flow system, northeastern coast of the Yucatan Peninsula, *Ground Water*, 30(3), 343–350.
- Perrin, C., C. Michel, and V. Andreassian (2001), Does a large number of parameters enhance model performance? Comparative assessment of common catchment model structures on 429 catchments, *J. Hydrol.*, 242(3–4), 275–301.
- Quinn, J., and D. Tomasko (2000), A numerical approach to simulating mixed flow in karst aquifers, in *Groundwater Flow and Contaminant Transport in Carbonate Aquifers*, edited by I. D. Sasowsky and C. M. Wicks, pp. 147–156, A. A. Balkema, Brookfield, Vt.
- Sasowsky, I. D. (2000), Carbonate aquifers: a review of thoughts and methods, in *Groundwater Flow and Contaminant Transport in Carbonate Aquifers*, edited by I. D. Sasowsky and C. M. Wicks, pp. 1–14, A. A. Balkema, Brookfield, Vt.
- Tezcan, L. (1998), Distributed modeling of flow and transport dynamics in large scale karst aquifer system by environmental isotopes, report, 23 pp., Int. Atomic Energy Agency, Vienna.
- Van Ommen, H. C. (1985), The “mixing-cell” concept applied to transport of non-reactive and reactive components in soils and groundwater, *J. Hydrol.*, 78, 201–213.
- Wicks, C., and J. S. Herman (1995), The effect of zones of high porosity and permeability on the configuration of the saline-freshwater mixing zone, *Ground Water*, 33(5), 733–744.
- Worthington, S. R. H., G. J. Davies, and D. C. Ford (2000), Matrix, fracture and channel components of storage and flow in a Paleozoic limestone aquifer, in *Groundwater Flow and Contaminant Transport in Carbonate Aquifers*, edited by I. D. Sasowsky and C. M. Wicks, pp. 113–128, A. A. Balkema, Brookfield, Vt.

B. Arfib, Université de Provence Aix-Marseille I, Laboratoire Chimie et Environnement, case 29, 3 place Victor Hugo, 13331 Marseille cedex 3, France. (bruno.arfib@up.univ-mrs.fr)

G. de Marsily, UMR CNRS 7619 Sisyphe, Laboratoire de Géologie Appliquée, Université Pierre et Marie Curie, Paris VI, Case 105, 4 place Jussieu, 75252 Paris cedex 5, France.